Supplement of Biogeosciences, 23, 5055–5069, 2026
https://doi.org/10.5194/bg-23-5055-2026-supplement

Supplement of

Shifts in riverine POC sources reduce terrestrial OC burial in the Changjiang subaqueous delta

Jiyuan Jin et al.

Correspondence to: Ya Ping Wang (ypwang@nju.edu.cn) and Wei Feng (wfeng_2024@163.com)

S1 Data processing

S1.1 Medium grain size of SPM and surface sediment

The medium grain size of suspended particulate matter (SPM) and surface sediments is a key factor controlling organic carbon (OC) retention capacity. In this study, grain size values reported in phi (Φ) units in the compiled literature were converted to μm using Eq. (S1):

$$D\ (\mu m) = 2^{-\Phi} \times 1000 \qquad \text{(S1)}$$

where *D* represents the particle diameter (μm) of the sediment particle.

S1.2 $\Delta^{14}C$ in SPM and surface sediment

Radioactive ^{14}C levels serve as critical proxies for determining sediment age. In this study, the modern ^{14}C fraction ($F^{14}C$ or Fm) reported in some compiled studies was converted to $\Delta^{14}C$ according to Stuiver and Polach (1977) using Eq. (S2):

$$\Delta^{14}C\ (‰) = [F^{14}C \times e^{\lambda(1950-yr)} - 1] \times 1000 \qquad \text{(S2)}$$

where λ = 1/8267, and *yr* is the year of sample collection.

S2 Data calculation

S2.1 OC Burial efficiency and OC preservation efficiency in the Changjiang subaqueous delta

The OC burial efficiency (OCBE) and OC preservation efficiency (OCPE) at each sampling site are estimated based on the formula in the main text. To reduce the influence of unequal sample sizes among sedimentary facies, the OC burial efficiency and preservation efficiency in the entire Changjiang subaqueous delta was calculated based on Eq. (S3):

$$\overline{E}_{\mathrm{delta}} = \frac{1}{4}\left(\frac{1}{m}\sum_{i=1}^{m} E_{\mathrm{DF},i} + \frac{1}{n}\sum_{j=1}^{n} E_{\mathrm{PD},j} + \frac{1}{p}\sum_{k=1}^{p} E_{\mathrm{DS},k} + \frac{1}{q}\sum_{l=1}^{q} E_{\mathrm{SH},l}\right) \quad \text{(S3)}$$

where $\overline{E}_{delta}$ represents either OC burial efficiency or OC preservation efficiency, and the E_{DF} denotes either OC burial efficiency or preservation efficiency in Delta front and so on; and m, n, p, and q indicate the numbers of surface sediment samples from the Delta front, Prodelta, Delta–shelf and Shelf, respectively.

S2.2 Riverine OC flux and OC net preservation flux

According to the POC contents (wt% of dry sediment) in SPM and riverine sediment load in June and July from 2001 to 2020 (Fig. S8), as well as estimated OC preservation efficiency, we further evaluated the monthly riverine OC flux and amount of OC preservation according to Eqs. (S4) and (S5):

$$Riverine\ OC\ flux\ (t/month) = OC\ (\%)/100 \times monthly\ sediment\ flux\ (t/month) \tag{S4}$$

$$OC\ preservation\ flux\ (t/month) = OC\ (\%)/100 \times monthly\ sediment\ flux\ (t/month) \times OCPE\ (\%)/100 \tag{S5}$$

where the *Riverine OC flux* denotes the monthly riverine POC input into the Changjiang Estuary, and the *OC preservation* represents monthly budgets of OC preserved in the Changjiang subaqueous delta, and thus the difference between *OC flux* and *OC preservation* can be identified as amounts of OC loss. The data were primarily collected in June and July, thereby capturing a representative period of the riverine POC fluxes and nearshore OC budgets in the Changjiang Estuary during the flood season. This interval corresponds to the most dynamic phase of POC transport within the annual cycle.

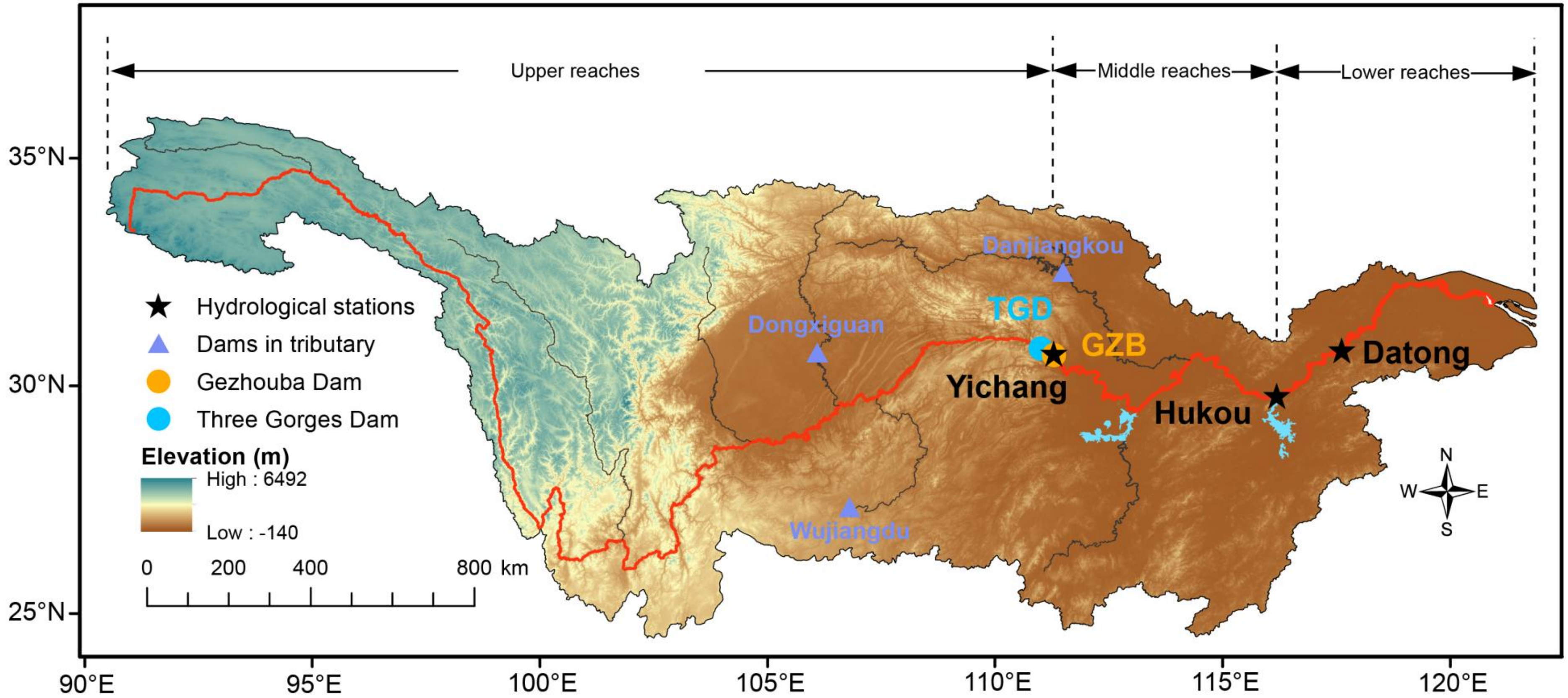

Fig. S1 Map of the Changjiang River Basin and locations of major dams constructed in mainstream and tributaries of the Changjiang River since 1965. Details of these dams are presented in Table S1. TGD: Three Gorges Dam, GZB: Gezhouba Dam.

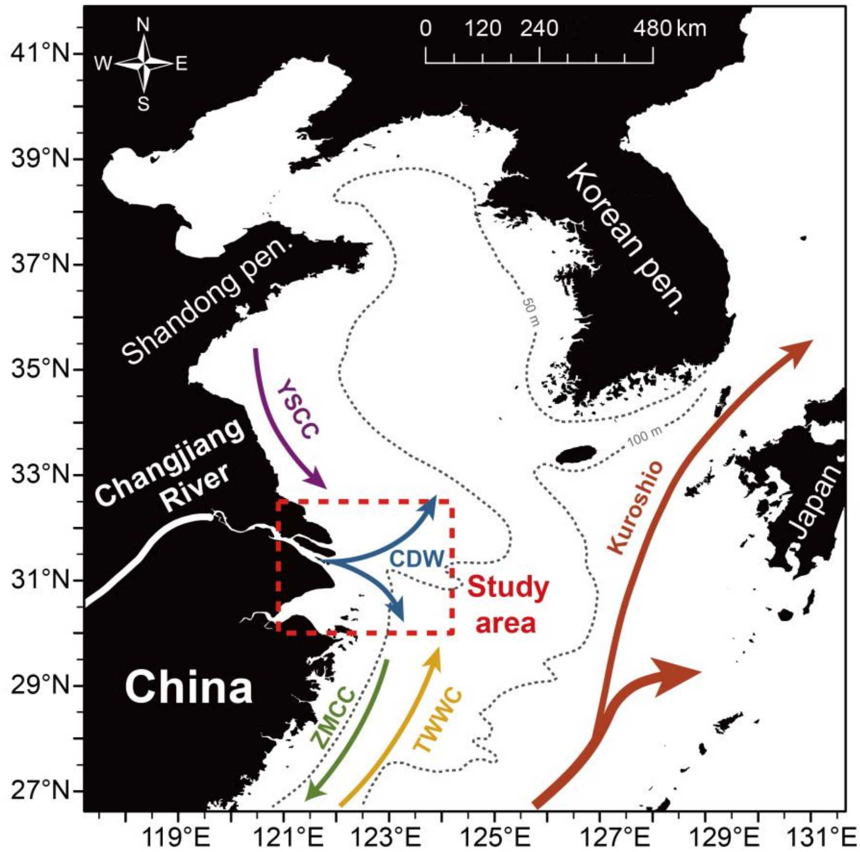

Fig. S2 Bathymetry and the major coastal and shelf circulation systems in the eastern Chinese marginal seas. YSCC, Yellow Sea Coastal Current; CDW, Changjiang Diluted Water; ZMCC, Zhejiang-Fujian Coastal Current; TWWC, Taiwan Warm Current. The circulation patterns were drawn based on previous studies (Xu et al., 2012; Yao et al., 2014; Feng et al., 2017; Lei et al., 2024; Sheng et al., 2024).

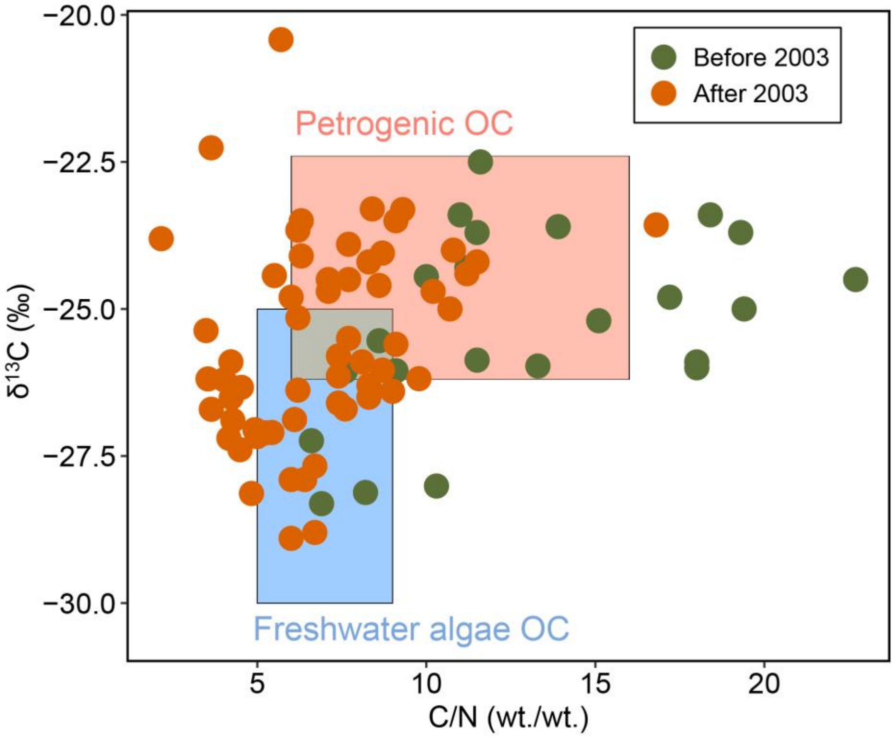

Fig. S3 Relationships between $\delta^{13}C$ and C/N in riverine suspended particulate matter (SPM) delivered by the Changjiang River. Light red and blue areas represent approximate ranges of $\delta^{13}C$ and C/N corresponding to terrestrial OC derived from petrogenic and freshwater algae OC sources, respectively, in terms of Lamb et al. (2006) and Menges et al. (2020). Note different colors of points indicate the samples collected in two periods (before 2003 and after 2003).

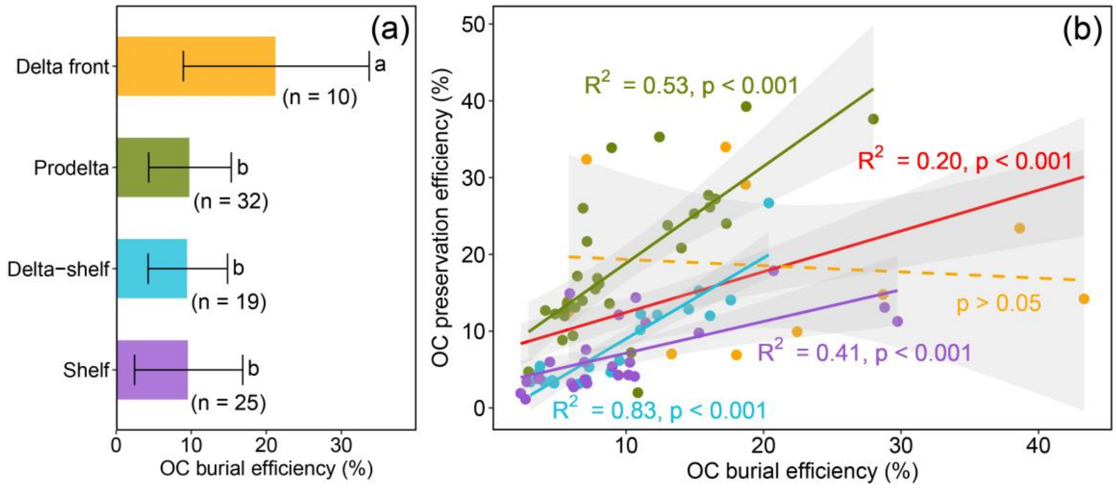

Fig. S4 Burial efficiency of terrestrial organic carbon (OC) in different sedimentary facies of the Changjiang subaqueous delta (a). Relationships between OC preservation efficiency and burial efficiency in different sedimentary facies (b). The solid and dashed lines represent statistically significant ($p < 0.05$) and non-significant ($p > 0.05$) relationships, respectively, and the light gray areas around the line indicate 95% confidence interval. Different colors in panel (b) represent different sedimentary facies (Yellow, Delta front; Green, Prodelta; Blue, Delta-shelf; Purple, Shelf), and the red line indicates relationships between OC preservation efficiency and burial efficiency for all points irrespective of sedimentary facies.

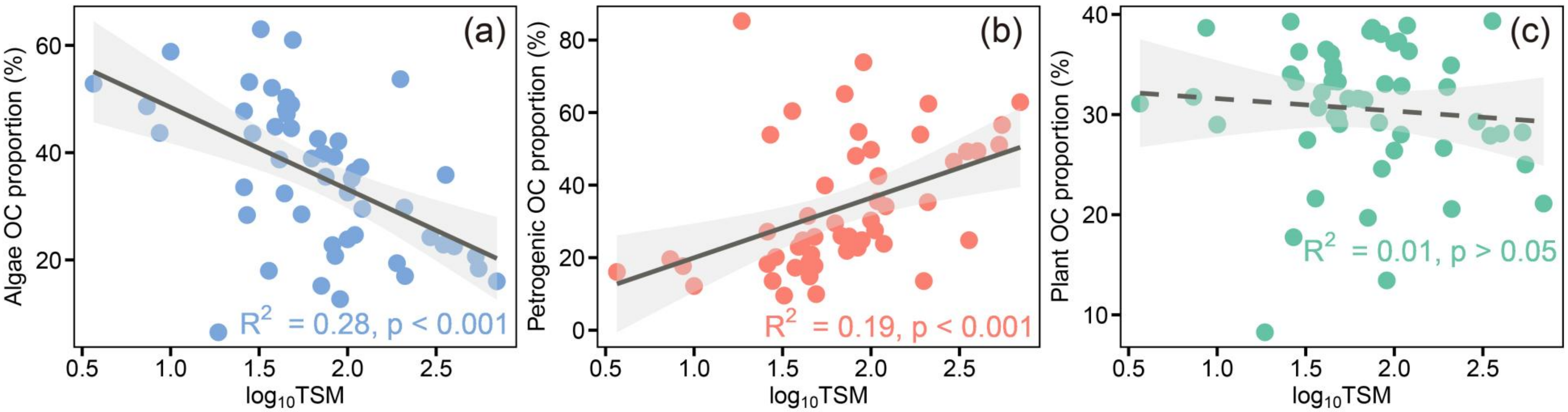

Fig. S5 Relationships between log-transformed total suspended matter (TSM) concentrations and proportion of algae (a), petrogenic (b) and C3 plant (c) OC sources. The solid and dashed lines represent statistically significant ($p < 0.05$) and non-significant ($p > 0.05$) relationships, respectively, and the light gray areas around the line indicate 95% confidence interval.

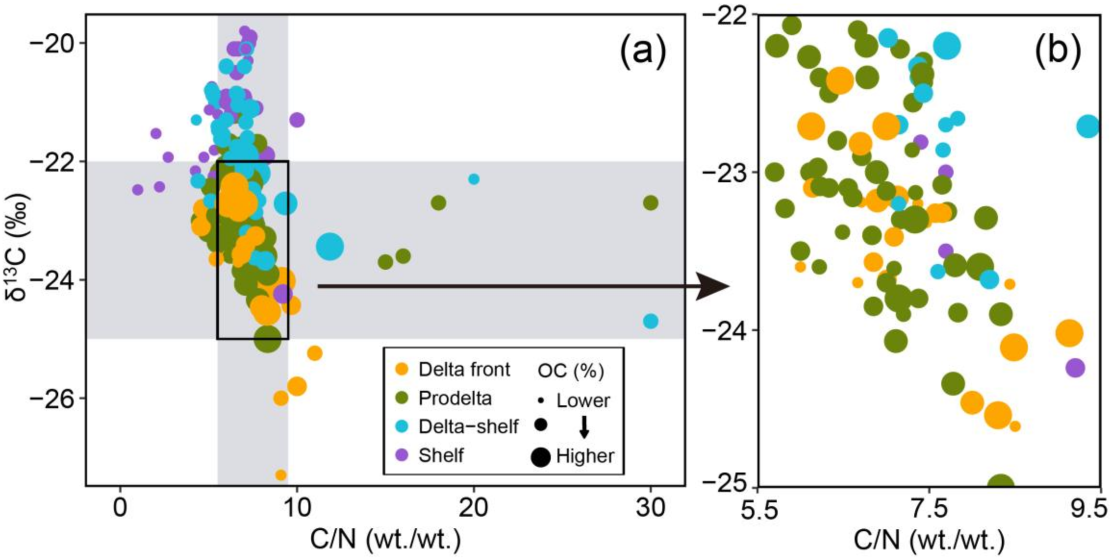

Fig. S6 Values of $\delta^{13}C$ versus C/N in bed sediments in different sedimentary facies of the Changjiang subaqueous delta (a), the light gray areas indicate approximate ranges of $\delta^{13}C$ and C/N characterized by higher OC contents. Details of the delimited area are amplified in panel (b).

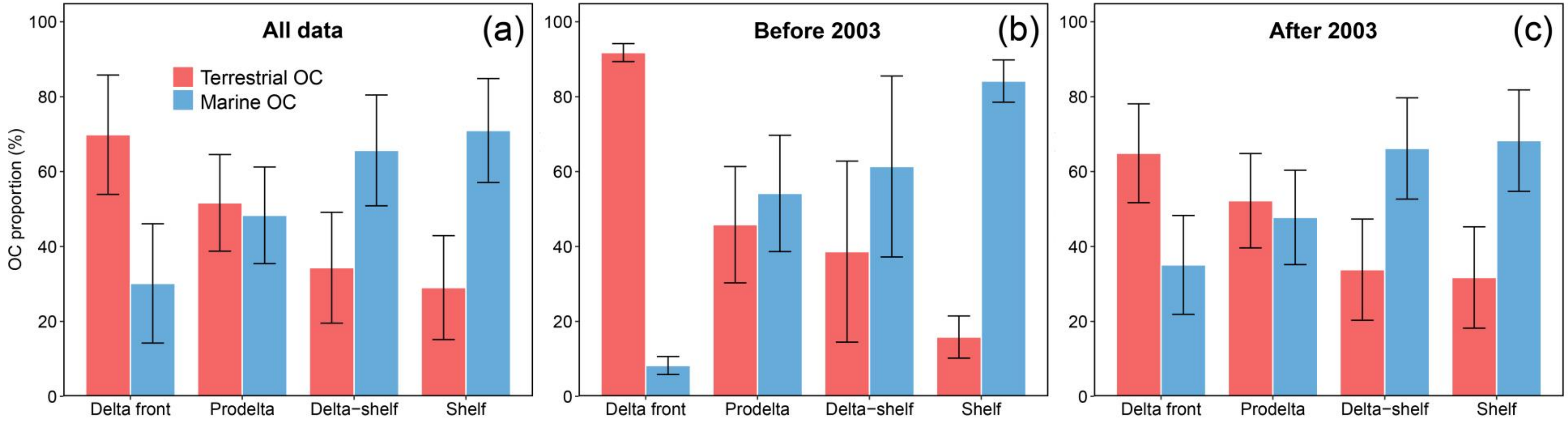

Fig. S7 Proportion of terrestrial and marine organic carbon (OC) in surface sediments across four sedimentary facies, presented for (a) all data, (b) the period before 2003, and (c) the period after 2003.

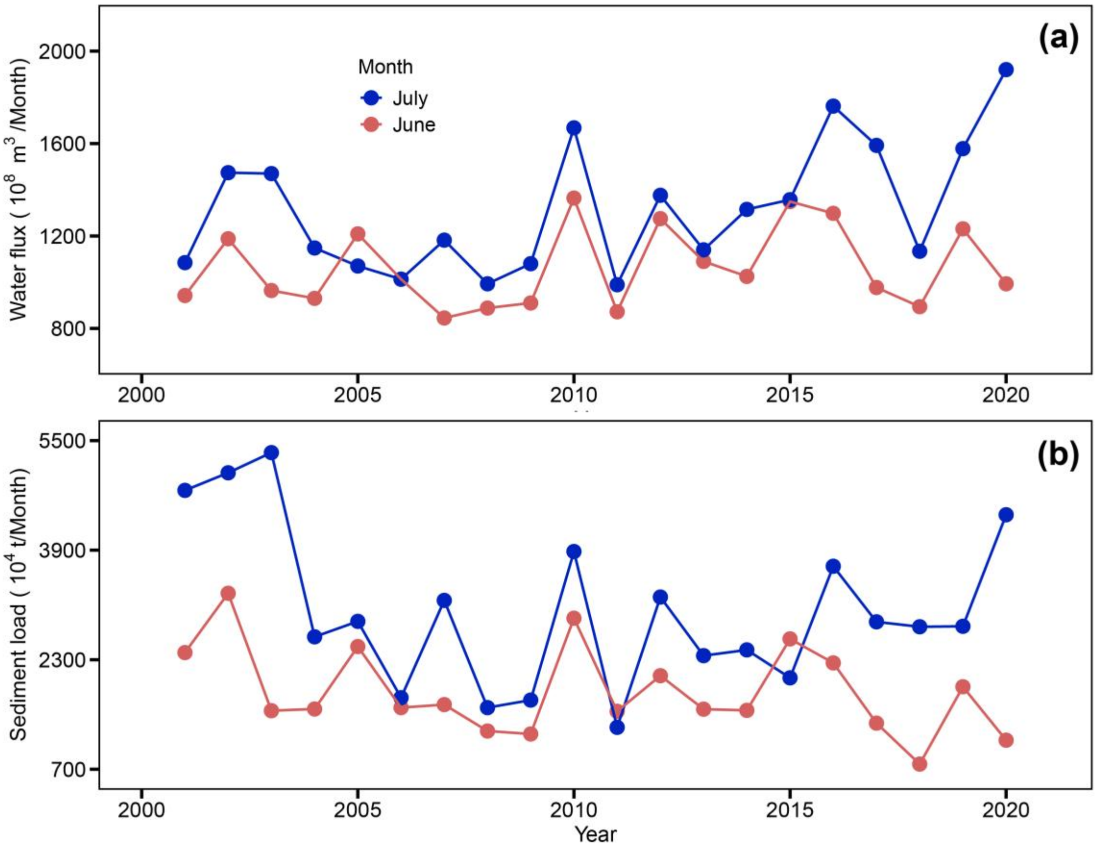

Fig. S8 Water flux (a) and sediment load (b) of the Changjiang River in June and July from 2001 to 2020 observed in Datong Gauge Station.

Table S1 Major reservoirs in main stream and tributaries of the Changjiang River operated since 1965.

Reservoir	**River**	**Commissioning year**	**Capacity (10^8 m^3)**
Danjiangkou	Hanjiang	1968	290.5
Wujiangdu	Wujiang	1979	23
Gezhouba	Main stream of the Changjiang River	1981	15.8
Dongxiguan	Jialingjiang	1996	5.98
Three gorges	Main stream of the Changjiang River	2003	450.4

Table S2 Endmember values of $\delta^{13}C$ and N/C molar ratios from terrestrial and river autochthonous sources of particulate organic carbon (POC) in riverine suspended particulate matters (SPM).

POC sources in SPM	$\delta^{13}C$ (‰)	N/C (molar ratio)
Algae	-28.5 ± 2[a]	0.184 ± 0.011[b]
Petrogenic	-22.4 ± 4.9[c]	0.045 ± 0.066[d]
C3 Plant	-26.8 ± 0.1[e]	0.038 ± 0.019[b]

[a] Shan et al. (2021).

[b] Tao et al. (2009), Ru et al. (2020) and Zhang et al. (2022).

[c] Aucour et al. (2006), Li et al. (2018) and Wang et al. (2019).

[d] Cremonese et al. (2014) and Menges et al. (2020).

[e] Sun et al. (2021).

Table S3 Characteristics of various parameters, as well as contents of different sources of particulate organic carbon (POC) separated from Bayesian end-member mixing model in suspended particulate matters (SPM) delivered by the Changjiang River. The values represent mean ± standard error. PN, particulate nitrogen.

Sampling date	POC (%)	PN (%)	C/N (wt./wt.)	$\delta^{13}C$ (‰)	Algae OC (%)	Petrogenic OC (%)	C3 Plant OC (%)
June 1980			12.93 ± 1.17	-23.5 ± 0.24			
November 1981			18.38 ± 1.03	-25.0 ± 0.36			
July 2001	0.95 ± 0.25	0.10 ± 0.04	9.22 ± 0.64	-26.6 ± 0.41	0.34 ± 0.08	0.25 ± 0.09	0.34 ± 0.08
June 2011	0.87 ± 0.09	0.08 ± 0.01	11.05 ± 0.19	-24.4 ± 0.22	0.18 ± 0.03	0.43 ± 0.02	0.25 ± 0.04
March 2012	0.69 ± 0.04	0.07 ± 0.01	10.73 ± 1.54	-24.3 ± 0.49	0.14 ± 0.02	0.36 ± 0.06	0.18 ± 0.02
July 2013	1.06 ± 0.06	0.15 ± 0.03	7.33 ± 0.71	-24.3 ± 0.26	0.23 ± 0.04	0.55 ± 0.01	0.28 ± 0.03
July 2014	1.11 ± 0.09	0.14 ± 0.01	8.18 ± 0.27	-25.0 ± 0.49	0.31 ± 0.06	0.44 ± 0.05	0.35 ± 0.06
July 2018	0.87 ± 0.13	0.12 ± 0.02	7.18 ± 0.55	-24.7 ± 0.67	0.23 ± 0.09	0.38 ± 0.04	0.26 ± 0.08
July 2019	4.01 ± 0.80	0.65 ± 0.14	6.35 ± 0.21	-25.2 ± 0.93	1.27 ± 0.41	1.56 ± 0.45	1.18 ± 0.33
June 2020	2.20 ± 0.80	0.34 ± 0.13	6.81 ± 0.56	-28.0 ± 0.45	1.22 ± 0.44	0.28 ± 0.11	0.70 ± 0.26
March 2021	1.02 ± 0.07	0.13 ± 0.01	7.73 ± 0.27	-25.5 ± 0.40	0.31 ± 0.05	0.36 ± 0.04	0.35 ± 0.05
March 2025	1.28 ± 0.19	0.25 ± 0.03	5.25 ± 0.54	-26.7 ± 0.31	0.60 ± 0.10	0.25 ± 0.04	0.42 ± 0.07
July 2025	1.70 ± 0.28	0.35 ± 0.07	3.84 ± 0.25	-25.8 ± 0.51	0.73 ± 0.15	0.44 ± 0.06	0.53 ± 0.11

Table S4 Characteristics of various parameters in riverine suspended particulate matter (SPM) and different sedimentary facies of the Changjiang subaqueous delta. The values represent mean ± standard error. OC, organic carbon; TN, total nitrogen; SA, specific surface area; MGS, medium grain size.

	OC (%)	**TN (%)**	**C/N**	**$\delta^{13}C$ (‰)**	**$\Delta^{14}C$ (‰)**	**SA (m^2/g)**	**OC/SA (mg C/m^2)**	**MGS (μm)**
Riverine SPM								
Summer	1.67 ± 0.20	0.26 ± 0.04	7.91 ± 0.41	-25.5 ± 0.24	-291.4 ± 18.3	14 ± 1.40	2.4 ± 0.71	9.78 ± 0.90
Winter	1.07 ± 0.11	0.17 ± 0.02	10.17 ± 1.11	-25.6 ± 0.25				29.33 ± 5.61
Surface sediment in different sedimentary facies								
Delta front	0.50 ± 0.05	0.07 ± 0.01	8.01 ± 0.30	-24.3 ± 0.24	-495.3 ± 42.8	8.52 ± 2.02	0.63 ± 0.09	64.41± 14.17
Prodelta	0.52 ± 0.02	0.08 ± 0.00	7.52 ± 0.44	-22.9 ± 0.09	-344.4 ± 17.0	15.28 ± 0.83	0.42 ± 0.03	26.46 ± 5.67
Delta-shelf	0.37 ± 0.03	0.06 ± 0.00	7.53 ± 0.63	-21.8 ± 0.13	-382.9 ± 33.1	6.96 ± 0.46	0.57 ± 0.04	132.24 ± 11.41
Shelf	0.25 ± 0.02	0.04 ± 0.00	6.23 ± 0.30	-21.4 ± 0.13	-350.3 ± 23.6	5.57 ± 0.52	0.64 ± 0.05	321.0 ± 59.14

References

Aucour, A.M., France-Lanord, C., Pedoja, K., et al., 2006. Fluxes and sources of particulate organic carbon in the Ganga-Brahmaputra river system. Global Biogeochem. Cy. 20, GB2006.

Cremonese, L., Shields-Zhou, G.A., Struck, U., et al., 2014. Nitrogen and organic carbon isotope stratigraphy of the Yangtze Platform during the Ediacaran–Cambrian transition in South China. Palaeogeogr. Palaeocl. 398, 165–186.

Feng, Z.B., Liu, B.H., Zhao, Y.X., et al., 2017. Structure, distribution, and evolution history of the Early Holocene erosional mud ridge system on the inner East China Sea shelf near the Yangtze River estuary. Geomorphology 283, 173–188.

Lamb, A.L., Wilson, G.P., Leng, M.J., 2006. A review of coastal palaeoclimate and relative sea-level reconstructions using δ13C and C/N ratios in organic material. Earth-Sci. Rev. 75, 29–57.

Lei, S.P., Bu, D.Z., Guo, X.H., et al., 2024. Mitigation of hypoxia and ocean acidification on the inner East China Sea shelf impacted by the 2023 summer drought. Mar. Pollut. Bull. 207, 116830.

Li, B.Y., Zhang, D.W., Pang, X.Q., et al., 2018. Paired δ^{13}Ccarb and δ^{13}Corg records of the Ordovician on the Yangtze platform, South China. Aust. J. Earth Sci. 65, 809–822.

Menges, J., Hovius, N., Andermann, C., et al., 2020. Variations in organic carbon sourcing along a trans-Himalayan river determined by a Bayesian mixing approach. Geochim. Cosmochim. Acta 286, 159–176.

Ru, H.J., Li, Y.F., Sheng, Q., et al., 2020. River damming affects energy flow and food web structure: a case study from a subtropical large river. Hydrobiologia 847, 679–

695.

Shan, S., Luo, C.L., Qi, Y.Z., et al., 2021. Carbon isotopic and lithologic constraints on the sources and cycling of inorganic carbon in four large rivers in China: Yangtze, Yellow, Pearl, and Heilongjiang. J. Geophys. Res. Biogeo. 126, e2020JG005901.

Sheng, H., Darby, S.E., Zhao, N., et al., 2024. Anthropogenic eutrophication and stratification strength control hypoxia in the Yangtze Estuary. Commun. Earth Environ. 5, 235.

Stuiver, M., Polach, H.A., 1977. Discussion Reporting of ^{14}C Data. Radiocarbon 19, 355–363.

Sun, X.S., Fan, D.J., Chen, P., 2021. Source, transport and fate of terrestrial organic carbon from Yangtze River during a large flood event: Insights from multiple-isotopes (δ^{13}C, δ^{15}N, Δ^{14}C) and geochemical tracers. Geochim. Cosmochim. Acta 308, 217–236.

Tao, F.X., Liu, C.Q., Li, S.L., 2009. Source and flux of POC in two subtropical karstic tributaries with contrasting land use practice in the Yangtze River Basin. Appl. Geochem. 24. 2102–2112.

Wang, J., Hilton, R.G., Jin, Z.D., et al., 2019. The isotopic composition and fluxes of particulate organic carbon exported from the eastern margin of the Tibetan Plateau. Geochim. Cosmochim. Acta 252, 1–15.

Xu, K., Li, A., Liu, J.P., et al., 2012. Provenance, structure, and formation of the mud wedge along inner continental shelf of the East China Sea: A synthesis of the Yangtze dispersal system. Mar. Geol. 291, 176-191.

Yao, P., Zhao, B., Bianchi, T.S., 2014. Remineralization of sedimentary organic carbon in mud deposits of the Changjiang Estuary and adjacent shelf: Implications for carbon preservation and authigenic mineral formation. Cont. Shelf Res. 91, 1–11.

Zhang, J., Guo, Q.J., Wang, Z.T., et al., 2022. Phytoplankton dominates the suspended particulate nitrogen source in the Yangtze River. J. Hydrol. 615, 128607.